

# Determination of the Jet Energy Scale

Sven Menke<sup>a</sup>

<sup>a</sup>Max-Planck-Institut für Physik, Föhringer Ring 6, 80805 München, Germany

The uncertainty in jet energy scale is one of the dominating systematic errors for many measurements at hadron colliders – most notably for the measurement of the top-quark-mass, inclusive jet cross section measurements and last but not least for events with large missing transverse energy as expected in searches beyond the standard model. This talk will review the approaches taken at Tevatron towards controlling the jet energy scale and discuss prospects for the LHC experiments.

## 1. Introduction

Jet energy calibration can roughly be divided in 4 steps:

### Tower and/or cluster reconstruction

Based on the smallest calorimeter readout objects (cells or towers) the input for jets are formed as fixed size towers or variable size clusters. The latter allow for shower containment and shape studies, the former guarantee a small size throughout the acceptance. Relevant for the later jet calibration is the level of noise- and pile-up-suppression (often referred to as zero-suppression) applied to the calorimeter readout channels. Comparisons of events with and without zero-suppression are needed to measure the residual background inside jets.

**Jet making** The input is grouped in jets defined by proximity in  $\Delta\eta \times \Delta\phi$  and/or relative transverse momentum. Mainly different cone-type [1] and **kT**-type [2–4] jet algorithms are in use at Tevatron and LHC. Common to all of them is the ability to run on any object with 4-vector interface (cell, tower, cluster, track, particle, parton), which allows for comparing jets reconstructed on different levels (e.g. calorimeter jets made of towers with MC truth jets made of stable particles). Typical cone radii in  $\Delta\eta \times \Delta\phi$ -space range from  $R = 0.4$  to  $R = 1.0$  and most modern implementa-

tions of cone algorithms address infrared and collinear safety. The final jet energy scale is jet-algorithm and size dependent but the general calibration strategies are independent of the actual algorithm and simply repeated for each jet type.

### Calibration to stable particle level

Instrumental effects like shower containment, noise, and calorimeter response are accounted for at this stage. The resulting particle jets can already be used for measurements, comparisons with other experiments and theory.

**Calibration to parton level** Depending on the analysis and physics channel a final correction to the originating parton (quark or gluon) is needed. Effects like hadronization, fragmentation, flavor-dependency and gluon radiation are taken into account.

## 2. Calibration Approaches

Jets can be either calibrated by applying one or more correction functions directly on the jet-level (i.e. depending on the 4-vector of the jet) or by calibrating the constituents (cells, towers, or clusters) and re-calculating the jet energy from the calibrated constituents. The final calibration from particle to parton level is applied on the jet 4-vector in both cases. The current schemes of the four experiments are:

**CDF** The particle level corrections for the jet in

$p_{\perp}$  are given by [5]:

$$p_{\perp}^{\text{ptcl}} = (p_{\perp}^{\text{raw}} \times C_{\eta} - C_{\text{MI}}) \times C_{\text{Abs}}, \quad (1)$$

where  $p_{\perp}^{\text{raw}}$  denotes the transverse jet momentum on the calorimeter scale,  $C_{\eta}$  corrects for non-uniformities in  $\eta$  based on simulated di-jet events,  $C_{\text{MI}}$  removes offset energy inside the jet cone due to pile-up,  $C_{\text{Abs}}$  scales the jet to the particle level based on di-jet simulations with mapped response from matched truth particle jet and calorimeter jet pairs, and  $p_{\perp}^{\text{ptcl}}$  is the corrected transverse jet momentum on particle level. The corrections are mainly simulation driven after tuning the simulation to accurately describe the data and uncertainties are derived from validation samples in various physics channels (di-jet,  $\gamma$  + jet, single particles).

**DO** The energy of the particle jet is given by [6, 7]:

$$E^{\text{ptcl}} = \frac{E^{\text{raw}} - O}{F_{\eta} \times R \times S}, \quad (2)$$

where  $E^{\text{raw}}$  is the jet energy on the calorimeter scale,  $O$  accounts for energy offsets due to noise and pile-up,  $F_{\eta}$  corrects for non-uniformities in  $\eta$  based on di-jet events,  $R$  scales the jet to the particle level based on  $\gamma$  + jet events,  $S$  corrects for the shower containment, and  $E^{\text{ptcl}}$  is the corrected jet energy on particle level. The corrections are mainly in-situ driven and separately derived for data and simulation.

**CMS** A modular scheme similar to that of the Tevatron experiments is currently favored [8], while the starting point at initial data taking will be Monte Carlo based calibration functions [9]. Another scheme under study uses separately clustered but matched deposits in the electromagnetic and hadronic sections which are classified as "em-like", "hadron-like", or "mip-like" based on the ratio  $E_{\text{had}}/E_{\text{em}}$  and

calibrated according to single particle response [10].

**ATLAS** The energy calibration to particle level is currently done in two different schemes [11]. In the first via global calibration functions [12] derived from  $\chi^2$ -fits of di-jet simulations with matched calorimeter and particle jets, where weights are applied to the individual cell level depending on the energy density [13] or to the sum of energy deposits in each sampling. The second, local hadron calibration method, classifies 3d topological clusters [14] as "em-like" or "hadron-like" by means of cluster shape variables and applies H1-style weights [15] derived from single pion simulations to the cells to account for non-compensation, and out-of-cluster weights on the cluster level to account for energy deposits in non-clustered cells. In both methods additional corrections for energy losses in front or in between samplings are applied, again either on global jet or local cluster level.

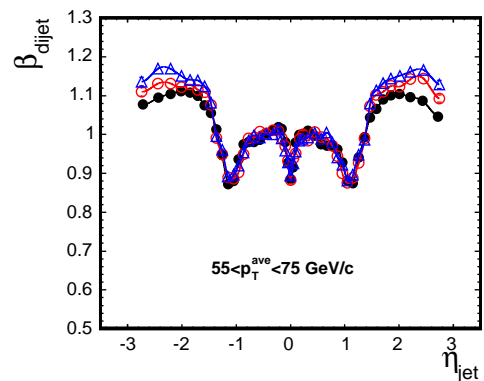


Figure 1. Di-jet balance for cone jets ( $R = 0.7$ ) with  $55 \text{ GeV} < p_{\perp} < 75 \text{ GeV}$  as function of the probe jet pseudo-rapidity  $\eta_{\text{jet}}^3$  for CDF Run II [5]; solid points show data, open triangles Herwig, and open circles Pythia.

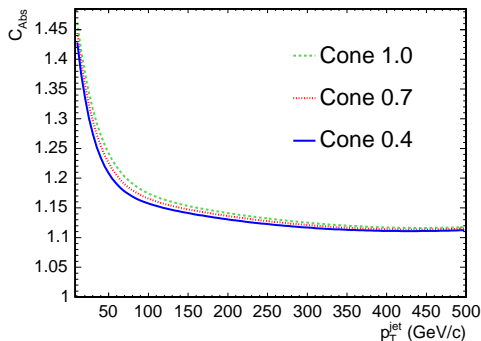


Figure 2. Absolute jet energy corrections for different cone sizes as function of the uncorrected jet transverse momentum  $p_{\perp}^{\text{jet}}$  for CDF Run II [5].

For the simulation driven calibrations the first step is to understand the calorimeter response to single particles and to tune the Monte Carlo accordingly. Either Geant4 and/or GFlash based simulations are in use and compared to beam test data and/or isolated single particles from minimum bias events.

The most widely used sample to correct for non-uniformities in  $\eta$  is QCD  $2 \rightarrow 2$  processes where back-to-back requirements in  $\phi$  for the two leading jets and strict upper bounds on the energy of the sub-leading jets ensure that  $p_{\perp}$ -balance arguments hold. CDF uses the  $p_{\perp}$ -balancing fraction  $f_b = \Delta p_{\perp} / \bar{p}_{\perp}$  of a central trigger jet and a probe jet to determine the correction function  $C_{\eta} = (2 + \langle f_b \rangle) / (2 - \langle f_b \rangle)$ , which is shown in Figure 1.

D0 uses the Missing  $E_{\perp}$  Projection Fraction method (MPF) on similarly selected di-jet events to obtain the inverse  $\eta$ -correction  $F_{\eta} = 1 + (\vec{E}_{\perp} \cdot \vec{n}_{\text{central jet}}) / E_{\perp \text{ central jet}}$ .

For the absolute scale di-jet simulations with matched particle and relatively corrected calorimeter jets are used in CDF. In D0 the MPF method is used again but this time on  $\gamma + \text{jet}$  events, where the fully reconstructed  $\gamma$  drives the absolute scale. Since only  $E_{\gamma}$  and  $E_{\perp}$  enter the MPF method the scale is independent of the jet-

size but requires additional shower containment corrections for jets. Figure 2 shows the magnitude of the absolute energy scale corrections ranging from about 10% at high  $p_{\perp}$  to about 50% at low  $p_{\perp}$ . Both relative and absolute scale are

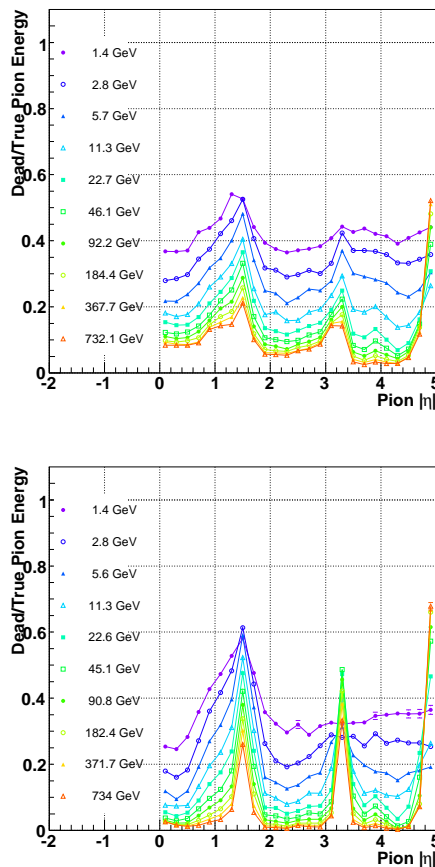


Figure 3. Energy deposits in dead material in ATLAS from single pion simulations at various energies vs.  $|\eta|$ . The upper plot shows charged pions, the lower plot neutral pions.

taken care of at once in the cell or sampling level global weighting approaches in ATLAS. The cell weights are functions of cell energy density and

derived for each sampling separately, where the jet energy dependency enters either as another argument or is taken care of in a separate jet-level correction. The cell weights in the local hadron calibration approach take a similar form but depend on the cell energy density and cluster energy instead of the jet energy and are derived from the ratio of total deposited energy in active and in-active material over reconstructed energy from single pion simulations. The major difference here is the treatment of individual small clusters as particle-like constituents after classifying them as "hadronic" or "electromagnetic" which allows to apply different type of weights to different parts of the jet.

The ATLAS approaches require additional corrections for the deposits in dead material which take the form of sampling energy dependent weights on the surrounding samplings and are applied on jet or cluster level. The local hadron calibration allows again to separately correct "electromagnetic" and "hadronic" clusters, to account for the different amount of dead-material deposits from neutral and charged pions as is shown in Figure 3.

If not included already in the applied corrections any cut-offs on the shower containment due to the finite jet-cone size need to be corrected for. D0 separates this effect from physics out-of-cone effects such as particles radiated outside the jet-acceptance by looking at the energy deposited in the calorimeter just outside the calorimeter-jet stemming from particles inside the corresponding particle-level jet. Similarly the ATLAS local hadron calibration corrects for finite shower containment on the cluster level taking the isolation degree of the cluster into account.

Residual noise, underlying event and pile-up contributions to the jets are subtracted from the jet energy in CDF and D0. The underlying event and residual noise activity can be measured in low luminosity minimum bias events using non-zero-suppressed random cones or  $\gamma$  + jet or di-jet events with cones in  $\phi$ -regions transverse to the main  $\phi$ -axis of the hard scatter. A measure of the pile-up contribution can be parameterized as a function of the number of observed vertices in minimum-bias events like is shown in Figure 4.

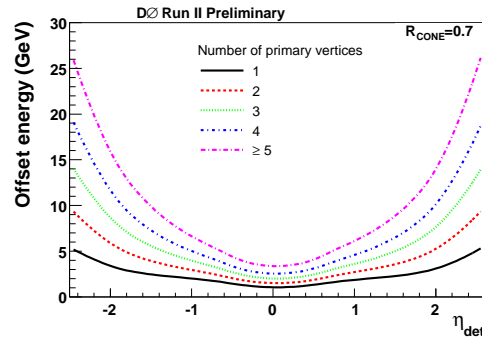


Figure 4. Offset energy for cone jets ( $R = 0.7$ ) as function of the jet pseudo-rapidity  $\eta_{\text{det}}$  for different numbers of primary vertices in D0 for Run II [7].

After the correction to particle level many analyses require to go back to the parton-level. CDF corrects for physics out-of-cone effects and underlying event offsets at this stage. The correction is derived from di-jet simulations as the ratio of the transverse momenta of a hard parton and the matched particle jet. A crucial step in this procedure is the validation in  $\gamma$  + jet-events with  $p_{\perp}$ -balance between parton-level corrected jet and photon energy. Data driven approaches use the  $p_{\perp}$ -balance in  $Z/\gamma$  + jet events directly to obtain the correction function to parton level. Also resonant decays like  $W \rightarrow q_i \bar{q}_j$  are used to establish the parton-level scale in-situ by virtue of a mass constraint or via template methods. For b-jets which have approximately a 5% lower response in the calorimeters additional corrections from direct comparisons to the parton level in simulated events are used, but also the  $p_{\perp}$ -balance in  $Z/\gamma$  + b-jet and  $Z$  + b-jet $\bar{b}$ -jet events with leptonically decaying  $Z$  are under study.

### 3. Uncertainties

The understanding of the jet energy scale reached a very mature level at Tevatron and uncertainties on  $p_{\perp}$  reach down to about 3% in the central region as is shown in Figure 5. The domi-

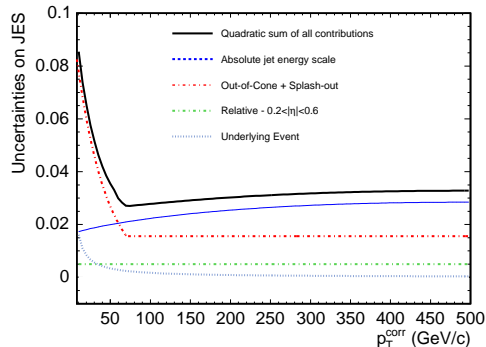


Figure 5. Total Uncertainties on the jet energy scale and the main contributions to it for central cone jets ( $R = 0.4$ ) as function of the corrected transverse jet momentum  $p_{\perp}^{\text{corr}}$  in CDF for Run II [5].

nant contributions at the high  $p_{\perp}$  end are from the absolute energy scale which is still limited by statistics – either single hadrons to validate the calorimeter simulation (CDF) or number of  $\gamma + \text{jet}$  events (D0). At low  $p_{\perp}$  the fluctuations in the out-of-cone or shower containment corrections contribute the largest uncertainty. Sizeable at low  $p_{\perp}$  are also the uncertainties introduced from the offset corrections for noise, pile-up and the underlying event, mainly due to residual luminosity dependency in each number-of-vertices bin. This will be even more substantial at LHC with expected number of multiple interactions  $\sim 10$ -times larger at design luminosity. The aim at the LHC experiments is to reach a 1% uncertainty level, but a more realistic number for the start is 4 – 5%.

#### 4. Conclusions

A general trend among all experiments is the modularization of different calibrations, each dealing with a different effect. The actual implementations are very different though – jet based or constituent based – Monte Carlo driven or relying on in-situ methods. For the LHC many options will be pursued in parallel and only the val-

idation with real data will tell us which ones are to be kept.

#### A. Acknowledgments

I'd like to thank the Jet Reconstruction and Jet Energy Scale groups of ATLAS, CDF, CMS, and D0 for providing me with the material presented here. In particular I benefited greatly from discussions with M. Bosmann, A. Juste, A. Kupco, P. Loch, M. D'Onofrio, C. Roda, N. Varelas.

#### REFERENCES

1. G. C. Blazey, et al., hep-ex/0005012.
2. S. D. Ellis, D. E. Soper, Phys. Rev. D48 (1993) 3160–3166.
3. S. Catani, Y. L. Dokshitzer, M. H. Seymour, B. R. Webber, Nucl. Phys. B406 (1993) 187–224.
4. M. Cacciari, G. P. Salam, Phys. Lett. B641 (2006) 57–61.
5. A. Bhatti, et al., Nucl. Instrum. Meth. A566 (2006) 375–412.
6. B. Abbott, et al., Nucl. Instrum. Meth. A424 (1999) 352–394.
7. J. Kvita, AIP Conf. Proc. 867 (2006) 43–50.
8. CMS Physics/Trigger Week: Jet Energy Scale Workshop, <http://indico.cern.ch/conferenceDisplay.py?confId=15200> (28 April 2007).
9. CMS Physics Technical Design Report Volume 1: Detector Performance and Software, CERN-LHCC-2006-001 (2006).
10. A. A. Bhatti, AIP Conf. Proc. 867 (2006) 425.
11. ATLAS Hadronic Calibration Workshop, <http://indico.cern.ch/conferenceDisplay.py?confId=13514> (26-27 April 2007).
12. ATLAS Detector and Physics Performance Technical Design Report, 1, CERN-LHCC-99-014 (1999).
13. W. Braunschweig, et al., Nucl. Instr. Meth. A265 (1988) 419.
14. C. Cojocaru, et al., Nucl. Instrum. Meth. A531 (2004) 481–514.
15. C. Issever, K. Borrás, D. Wegener, Nucl. Instrum. Meth. A545 (2005) 803–812.